



Geostatistical simulation and the health risk assessment of groundwater quality in south west of Iran

Mohamad Sakizadeh

Department of Environmental Sciences, Faculty of Sciences, Shahid Rajaee Teacher Training University, Tehran, Iran, Tel./Fax: +98 2122970005 Ext. 2358; email: msakizadeh@gmail.com

Received 13 October 2016; Accepted 14 May 2017

ABSTRACT

A study was conducted on the health risk of nitrate in groundwater resources (e.g., wells and springs) of an area in south west of Iran using two data records gathered in 2010 and 2011 years. It was concluded that at the moment, children are more exposed to higher than normal values of nitrate due to consumption of drinking water. In order to estimate the health risk of nitrate, a risk curve was constructed indicating that the number of residents exposed to groundwater with higher than 45 mg/L nitrate level fluctuated between 7,868 and 15,024 people with a mean value of 11,213 people. Geostatistical simulation of nitrate was implemented by sequential Gaussian simulation (SGS) and collocated co-kriging simulation (CCS) of nitrate in 2011 using the data of 2010 as the secondary information. It was concluded that uncertainty in predictions can be reduced using CCS; however, it is less exact than its SGS counterpart.

Keywords: Health risk assessment; Risk curve; Sequential Gaussian simulation; Collocated co-simulation; Remote sensing

1. Introduction

Groundwater pollution has become a widespread problem especially in developing countries. Among groundwater contaminants, nitrate is more common in areas in which agricultural activity is prevalent [1,2]. Nitrate does not bind to soil particles, so, it easily leaches through soil column resulting in groundwater contamination [3]. The high solubility of this compound also contributes to its accumulation in groundwater [4]. Groundwater vulnerability to contamination is usually assessed through monitoring of nitrate [5] and it is used as an indicator of diffuse sources of pollution [6]. Apart from this, it poses a high risk to consumers especially where groundwater is the main source of drinking water [5]. The well-known methaemoglobinaemia disease in infants is the direct consequence of consumption of water with high levels of nitrate [7]. Moreover, some other symptoms such as gastrointestinal illness and abdominal pain in elders have also been attributed to higher than threshold values of nitrate [8]. Natural sources of nitrate may release values

up to 10 mg/L NO_3^- in groundwater; however, levels higher than this have been attributed to anthropogenic sources for instance application of fertilizers in agricultural area and septic systems [9]. The health risk assessment of nitrate is therefore an important issue which should be considered by environmental managers. In this field, health risk assessment of exposure to nitrate has been considered in previous researches [10–13]. One of the objectives of the current study is to evaluate the health risk of exposure to nitrate by consumption of groundwater for adults and children in an arid area in south west of Iran.

On the contrary, one of the methods for management of contaminated area is to distinguish regions with high risk of groundwater pollution. Maps of contaminated areas are a way to fulfil this goal. Until now, different geostatistical methods have been utilized for this purpose. The most applied one is the kriging technique [14], but, its shortcomings such as smoothing problem (e.g., over estimation of small values and underestimation of large values) [15] next to the incapability to account for incurred uncertainty in predictions have

refrained some of researches to use this method for spatial assessment of contaminated area. A practical alternative is to apply geostatistical simulation for this purpose [16]. One of the redeeming features of geostatistical techniques is uncertainty assessment of predicted values through generation of different realizations [17]. Moreover, in geostatistical simulations not only data values but spatial continuity of attributes (e.g., variogram and semivariograms) is also reproduced whereas, kriging methods are only capable to honor data values [18].

On the other hand, a negative side of common geostatistical procedures is steady-state assumption as temporal data cannot be incorporated into analysis in usual methods because they have been designed for handling of spatial attributes [19]; however, most of water quality monitoring schemes produce spatial-temporal data. To use geostatistical methods for such systems, attributes have to be averaged over the entire time period resulting in loss of a great deal of valuable information. Several practical alternatives have been proposed by researcher to handle this problem. One of the possible solutions rendered by Rouhani and Hall [20] involves three-dimensional variogram fitting assuming time as the third dimension. Another option for handling temporal data is to assume temporal data as random correlated functions and use linear model of coregionalization (LMC) [19,21,22] or bilinear model of coregionalization in case of multivariate time series [23]. In this respect, co-kriging has been applied in previous researches on temporal nitrate data to improve the estimation of undersampled times using data of more intensely sampled time period [19]. In the latest research, uncertainty in the predictions of co-kriging has been significantly reduced compared with that of kriging by a data set of 47 samples to improve the predictions of undersampled data represented by 27 and 28 collected samples in other time periods.

In the current study, a new algorithm known as collocated co-simulation will be utilized to reduce the uncertainty of predictions made by an undersampled nitrate data using a more densely sampled data record of the previous year. In addition, a method for the spatial health risk assessment of local residents that are exposed to nitrate contamination is also proposed and its uncertainty will be discussed as well. As far as the author knows, collocated co-simulation has not been used for assessment of contaminated area; however, there are few case studies in other fields of environmental science. For instance, uncertainty in prediction of soil water content was compared through sequential Gaussian simulation (SGS) and collocated co-kriging simulation (CCS) algorithms in northern part of France [24]. It was concluded that in case of uncertainty, the predictions made by CCS procedure are more reliable than its SGS counterpart.

2. Materials and methods

2.1. Study area, field and laboratory analysis

The study region, with an area of about 1,100 km², is located in south west of Iran and it is characterized by an arid area with hot summer and spring seasons. Andimeshk and Susa are the main residential areas along with some other growing rural areas in the region. The main land use is agriculture where it is one of the most important agricultural

centers of Iran. The application of agricultural fertilizers, poorly regulated landfill disposal and septic tanks are the main factors contributed to contamination of groundwater in recent years [25]. Since drinking needs of local residents in villages is totally obtained through groundwater resources, so, maintaining the quality of groundwater is of paramount importance. The groundwater samples were collected during two water quality surveys conducted in 2010 (45 samples) and 2011 (21 samples) from wells and springs. Following acidification of samples by nitric acid, they were kept cool (e.g., at 4°C) and transported to laboratory for nitrate analysis by spectrophotometric technique [26]. Given in Fig. 1, a map of study area overlaid with values of nitrate in 2010 and 2011 sampling results. In addition, descriptive statistics of nitrate values in 2010 and 2011 have been rendered in Table 1.

2.2. Health risk assessment of nitrate

The non-carcinogenic health risk of long-term exposure to nitrate was quantified in term of hazard quotient (HQ) by the well-known method developed by USEPA [27] and used by many other researchers [9,12] as follows:

$$HQ = \frac{CDI}{RfD} \quad (1)$$

$$CDI = \frac{C \times IR \times EF \times ED}{(BW \times AT)} \quad (2)$$

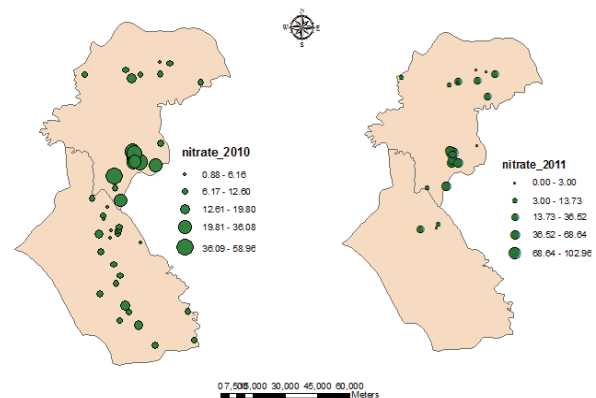


Fig. 1. A view of the study area with respect to the levels of nitrate in 2010 and 2011.

Table 1
Descriptive statistics of nitrate concentrations (mg/L) in 2010 and 2011

| Year | 2010 | 2011 |
|-----------------|-------|--------|
| Total samples | 45 | 21 |
| Minimum | 0.88 | 0.88 |
| Maximum | 58.96 | 102.96 |
| Average | 15.49 | 27.44 |
| SD ^a | 14.00 | 27.05 |

^aStandard deviation.

In which nitrate uptake through drinking sources is calculated by CDI while, RfD is the reference dose of nitrate which is equal to 1.6 mg/kg/d. Apart from the concentration of nitrate which is shown by C (mg/L) in the above equation, IR is the intake rate (1 L/d for children and 2 L/d for adults) whereas, the exposure frequency (EF) was 365 (d/year). The exposure duration (ED) was 6 years for children and 30 years for adults, respectively. The body weight (BW) of children and adults were selected as 20 and 60 kg, respectively, and average time (AT) of exposure for adults and children were 10,950 and 2,190 d, respectively. If the level of HQ exceeds one, it indicates a higher than normal health risk to water consumer.

In this study, a new method of risk assessment known as risk curve was also utilized to estimate the number of people exposed to higher than normal values of nitrate (e.g., 45 mg/L) in the study area. For this purpose, in each realization obtained through SGS (refer to conditional SGS) and each node, the predicted value of nitrate was compared with that of cut-off value of 45 mg/L. If the value exceeded, the number of inhabitants exposed to this level was retained in a spatial map otherwise, the number of exposed inhabitants was equal to zero. In the next step, the results were multiplied by the unit surface of the simulation grid to obtain the risk curve. Three different quantiles (including 5, 50 and 95) were applied to report the spatial risk of calculations as well.

2.3. Conditional sequential Gaussian simulation

In the current research, as the distribution of sampling points was more concentrated in some parts of the study area, so, the number of samples was declustered through a moving window by which a weight was assigned to each sample [28]. This weight was then used for Gaussian anamorphosis modeling by a mathematical function that transformed each variable (Y) to normal score values with a normal distribution (Z) (e.g., $Z = \Phi(Y)$). This is accomplished by fitting a polynomial expansion [29] through the following equation:

$$\Phi(Y) = \sum \Psi_i H_i(Y) \quad (3)$$

where H_i is a Hermite polynomial. The back transformation to original variable is then obtained by the inverse of this function (e.g., $Y = \Phi^{-1}(Z)$). More details about this modeling procedure can be found in Castrignanò et al. [28]. The variogram model was then fitted to the experimental semivariogram of normal score values. A simulation matrix comprised of 65×145 grids and a cell size of 1 km² was superimposed on the sampling stations to save the results. Each realization of simulated values was generated by defining a random path through grid nodes conditional on the original data and previously simulated values. This process was repeated until all of the nodes were visited. The simulated values were then converted to original space by the inverse of Gaussian anamorphosis function [30].

2.4. Conditional collocated co-simulation

Despite the SGS, in CCS the primary variable (nitrate of 2011) was simulated conditional to the both primary and secondary (nitrate 2010) information. The algorithm is similar to that of SGS except that co-kriging method is utilized to

compensate the problem of insufficient data provided that the secondary data is more densely sampled than that of the first one and has a high spatial correlation with the first attribute. Collocated co-kriging has the redeeming feature of being more exact and faster than that of simple co-kriging as well [31,32]. The other characteristics of CCS are the same as SGS and are not mentioned here for the sake of brevity. The advantage of collocated co-kriging over that of simple co-kriging is that, in this method, the estimations are performed without the need of fitting a LMC instead, the univariate variogram and collocated correlation between the first and secondary data are utilized for this purpose [33].

2.5. Land use map

To link agricultural and residential characteristics (e.g., the main contributing factors of nitrate contamination) of the study area to the levels of nitrate recorded in the region, it was decided to prepare a land use map using remote sensing images. For this purpose, two cloud free Landsat TM images (path = 166, row = 37 and 38) recorded in the same time in the July of 2010 were acquired. These images were obtained at level 1 T, meaning that they were geometrically corrected and orthorectified; however, the failure of scan line corrector introduced major striping in imagery which was corrected by gap-fill tool using a triangulation method. The main preprocessing step included conversion of digital numbers to radiance using gain and offset values for each band followed by the calibration of the image to top of the atmosphere reflectance using other calibration parameters (e.g., solar irradiance, solar elevation, acquisition time). As has been concluded in earlier studies, atmospheric correction is unnecessary in many applications involving land use classification and change detection as long as the training and classified data are in the same relative scale [34] while pansharpening plays a much more role than atmospheric correction [35]. Thus, the images were pansharpened using panchromatic band of the Landsat TM image through which the resolution was increased to 15 m while no atmospheric correction was applied on the images. Image mosaicing and extraction of the region of interest were the other preprocessings applied on the images. The classification of the image was implemented by overlaying seven training samples on the image represented as water bodies, vegetation, bare soil, residential area, mountainous area, forest and agriculture. In addition, separate sampling points were collected from the study area for the validation of the derived classification maps. The spectral separability of the training samples was assessed before classification to consider the extent of their statistical separability. The values fluctuate between 0 and 2 where values greater than 1.9 indicate good separability of pairs. In this study, the values ranged from 1.88 to 2 indicating reasonable separability of defined classes. Following the selection of training and validation samples, a supervised classification method using maximum likelihood technique [36] was carried out. The overall accuracy and kappa coefficient were used as criteria to assess the accuracy of the resultant classification image [37].

3. Results and discussion

Descriptive statistics associated with calculated HQs have been rendered in Table 2. Considering this table, the HQs

varied from 0.01 to 1.2 for adults in 2010, while it fluctuated between 0.02 and 1.8 at the same time period for children in the study area. On the contrary, local residents experienced a higher risk based on the results of HQs worked out in 2011 in the region. HQs changed from 0.01 to 2.1 for adults and from 0.02 to 3.1 for children, respectively. Adults were also exposed to a lower risk based on the mean values obtained for them which were in turn 3.2 and 0.57 in 2010 and 2011, respectively, whereas, the mean values were 0.47 and 0.84 for children in 2010 and 2011, respectively.

It can be concluded that on average the health risk of nitrate in groundwater for local residents was not higher than the cut-off value of one; however, in some parts of the region both children and adults are exposed to higher than threshold value which may have some ramifications for them in long-term according to the maximum values obtained in this study. It should be noted that only 13 sampling stations collocated between 2010 and 2011, so, it cannot be concluded that the health risk has augmented during this short-time period but as a whole, in the area that was considered in 2011, people were exposed to a higher risk than that of 2010.

The spatial maps of HQs in 2010 were produced through calculation of experimental variograms for adults and children. Experimental isotropic variograms (to simplify the problem) were drawn using a lag value of 3,275 m over a distance of 10 lags for each variogram. Variogram models were then fitted to the experimental variograms as have been illustrated in Fig. 2.

The best fitted variogram was a cubic model and comprised of a range of 8,066.29 m and a sill of 0.07. Since the spatial continuity of HQs for both children and adults were the same, so, only the experimental variogram and the model fitted to the variogram of adults have been given in Fig. 2. HQs were then converted to normal score values using Gaussian anamorphosis functions, given in Fig. 3 as an example for the HQ of adults, followed by variogram fitting to normal score values.

The simulation of normal score values of HQs was implemented by SGS method. The quality of simulations was tested by reproduction of fitted variograms vs. original values as well as reproduction of data histograms [38]. Variograms of 20 realizations were overlaid with the variogram of HQs for adults and children, indicating that, the simulation method has been able to successfully reproduce the spatial continuity of original data (Fig. 4). The histogram of realizations #1, #5,

#10, #15 and #20 was selected to examine the quality of simulation against that of original values (Fig. 5).

It is obvious that there is no smoothing problem associated with generated realizations since the minimum and maximum values have been exactly honored because during

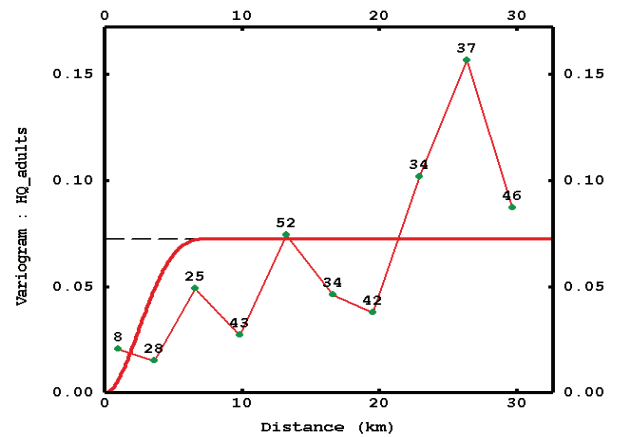


Fig. 2. Isotropic model fitted to experimental semivariogram of HQs for adults.

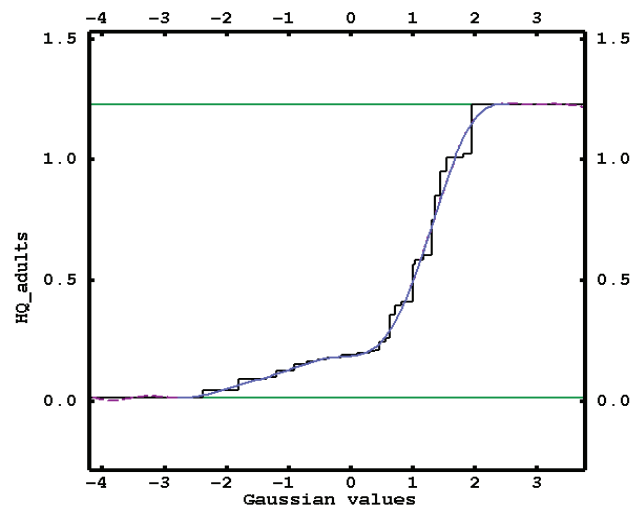


Fig. 3. An example of Gaussian anamorphosis function applied for conversion of HQs to normal score values.

Table 2
Descriptive statistics of calculated HQs in groundwater samples

| | 2010 | | 2011 | |
|---|-------------|---------------|-------------|---------------|
| | HQ (adults) | HQ (children) | HQ (adults) | HQ (children) |
| Minimum | 0.018333 | 0.026822 | 0.018333 | 0.026822 |
| Maximum | 1.228333 | 1.797068 | 2.145 | 3.138164 |
| Average | 0.322611 | 0.471984 | 0.57164 | 0.836317 |
| SD ^a | 0.291672 | 0.42672 | 0.563452 | 0.824339 |
| Number of samples | 45 | 45 | 21 | 21 |
| Number exceeding threshold ^b | 3 | 6 | 4 | 7 |

^aStandard deviation.

^bThreshold value is one.

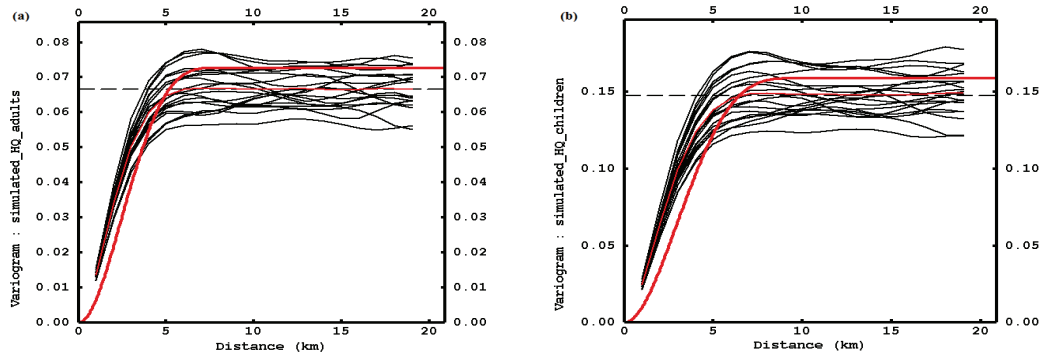


Fig. 4. Variograms of 20 realization superimposed on the variograms of HQs for adults (a) and children (b).

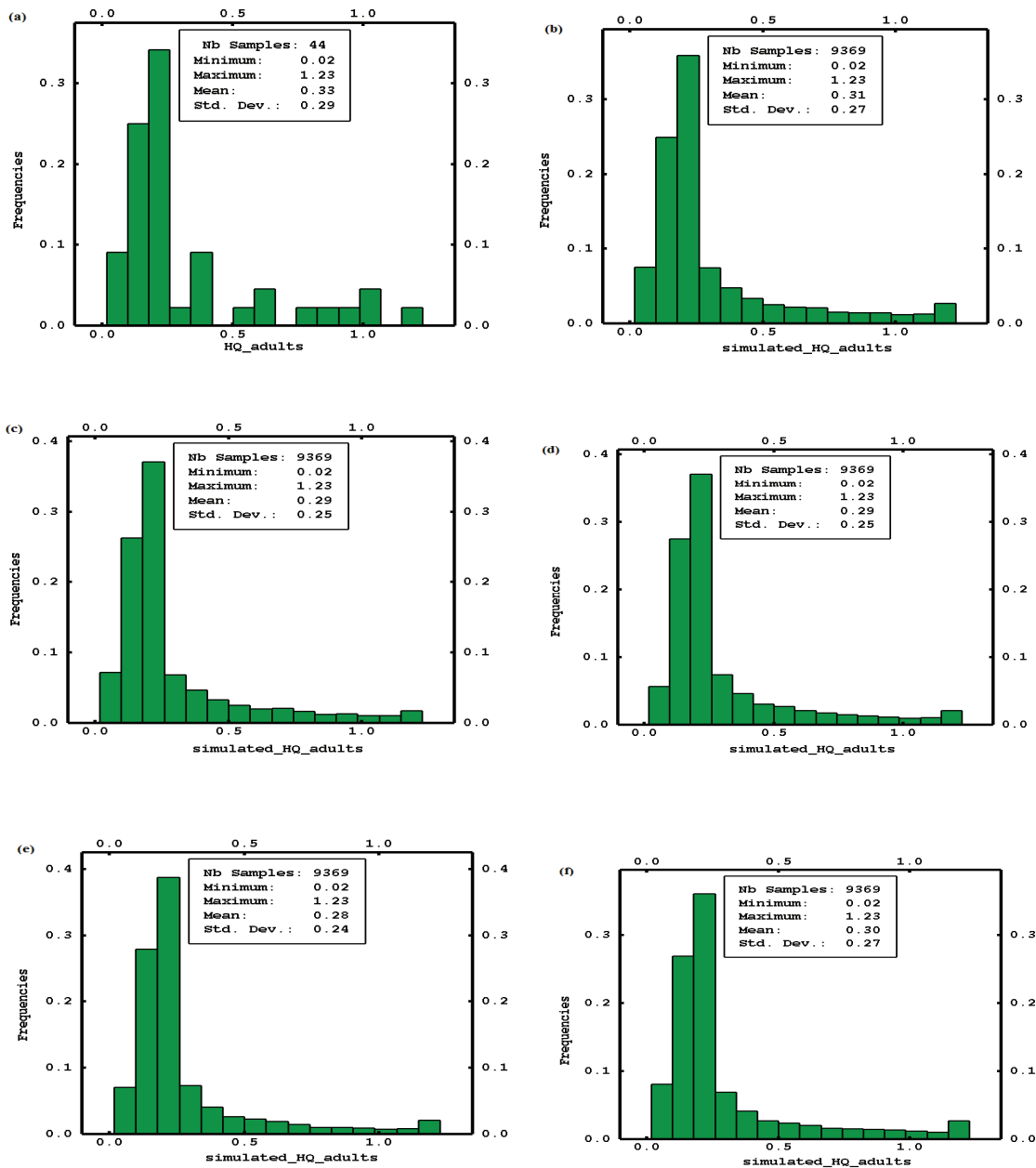


Fig. 5. Histogram of original adult HQ (a) vs. that of simulated HQs for realizations #1 (b), #5 (c), #10 (d), #15 (e) and #20 (f).

conditional simulation, the estimated values are conditional on original data as well as all previously simulated values [39]. Among the considered realizations, the best simulated histogram was related to simulation #1. As a whole, the data distribution has also been reproduced quit well. The mean and standard deviation of realizations for HQ of adults and children have been illustrated in Figs. 6(a) and (b). Considering the mean of realizations, the highest values of HQs are in the central part of the study area and have been highlighted using red colors. More specifically, the highest values are concentrated in Shahrak Azadi, Koy Lor and Koy Shohada districts.

A previous study on the vulnerability of groundwater to contamination in Andimeshk part of the study area using DRASTIC model (regarding parameters such as depth to

water table, topography, aquifer media, recharge, vadose zone, soil media) concluded that northern part of Andimeshk has a lower vulnerability to contamination compared with that of southern part [40] which is in agreement with the results of nitrate analysis in this study in which the highest nitrate values were found in the southern part of Andimeshk (Fig. 6).

As concluded earlier, children are more exposed to higher than normal values of HQs. The map of standard deviation indicates the uncertainty in predictions made through the mean of realizations. It is clear that there was a high uncertainty associated with the predictions in some areas in which the mean of realization was high as well. In order to reduce the uncertainty in the predictions, other algorithm was applied in this study and will be discussed later in the rest of this paper.

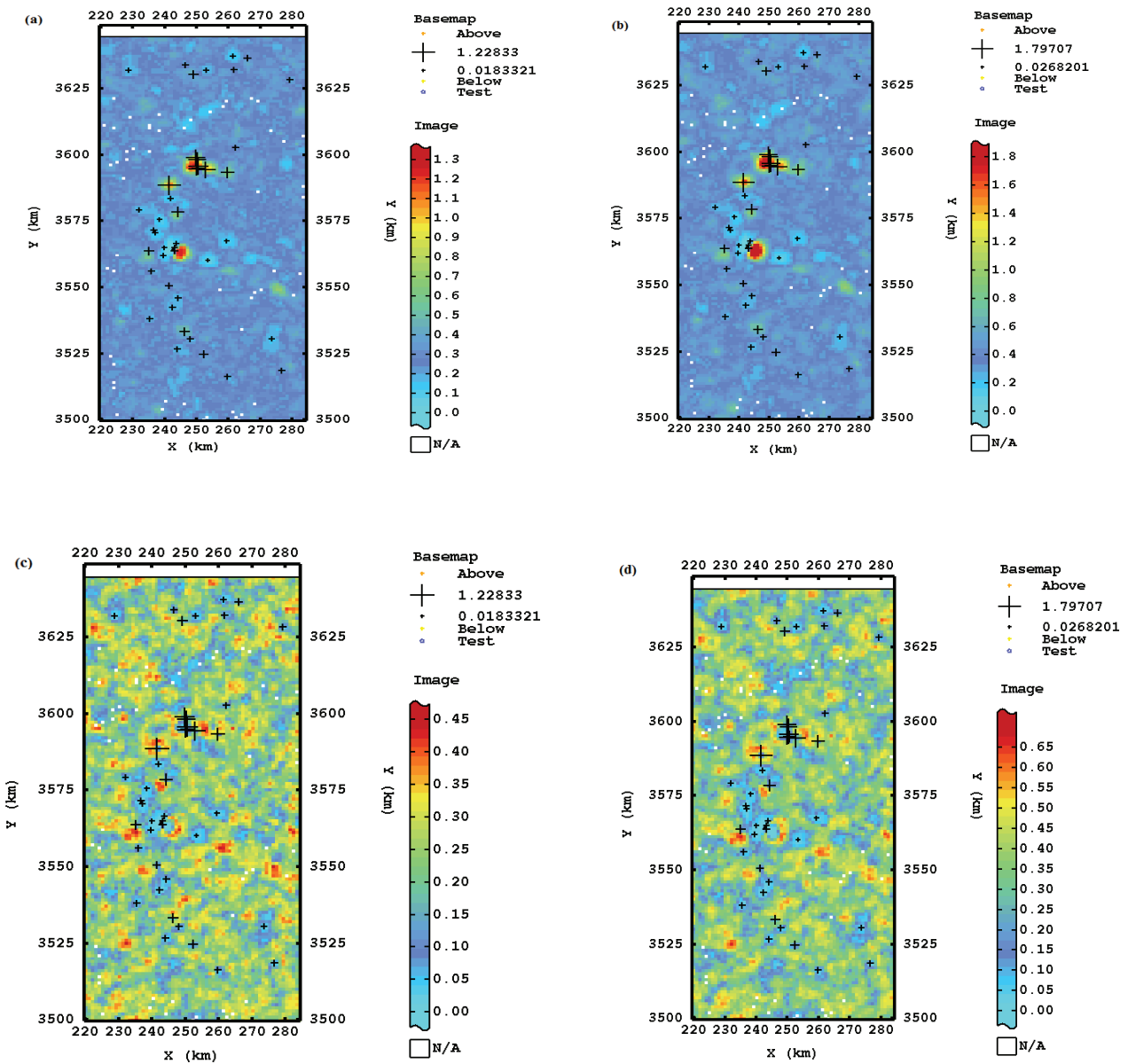


Fig. 6. Mean of realizations for simulated values of HQs for adults (a) and children (b) along with the standard deviation of simulated values for adults (c) and children (d).

The risk assessment was completed through generation of a risk curve in which the number of residents that are exposed to higher than threshold values of nitrate (e.g., 45 mg/L in this case) were estimated using the method explained earlier. For this purpose, a total number of 258 villages with a population of 134,817 people have been considered. The risk curve has been rendered in Fig. 7. With respect to this figure, the number of inhabitants exposed to groundwater with higher than 45 mg/L nitrate fluctuated between 7,868 and 15,024 people with a mean value of 11,213 people. The 5th, 50th and 90th quantiles of risk curves were 14,755, 10,984 and 8,331 people, respectively. In other words, in the worst case, about 11% of people and in the best case, about 6% of inhabitants are exposed to higher than normal values of nitrate.

As concluded earlier, there was a high uncertainty associated with the predicted values in areas in which the highest mean of realizations had been obtained. In this respect, Goovaerts [41] indicated that, the prediction errors can be reduced if we account for a second ancillary data as long as the correlation coefficients between the first and second data record is higher than 0.75. In the current study, the spatial correlation between the nitrate values in 2010 and 2011 in collocated stations (e.g., 13 out of 21 stations in 2011) was equal to 0.8, so, it was assumed that the prediction errors of nitrate in undersampled time frame in 2011 can be decreased by including the more comprehensive sampled data of 2010 in predictions using collocated co-simulation algorithm. To fulfil this goal, the experimental variogram of data of 2011 was first constructed. The variogram model was fitted through a cubic model with a range of 13,869.65 m and a sill of 526.5 (Fig. 8). Then the data were converted to normal score values by anamorphosis modeling and following fitting of variogram models they were simulated using both SGS and CCS algorithms.

The success of predictions was assessed through reproduction of experimental variograms, honoring data values and Quantile-Quantile (QQ) plots of predicted realizations selected at random vs. that of original attribute (e.g., nitrate of 2011). The reproduction of variogram was tested by overlapping the variograms of 20 realizations against that of original variogram for SGS and CCS algorithms (Fig. 9).

As has been shown in Fig. 9, the variogram of data was well reproduced through SGS algorithm, whereas, CCS has

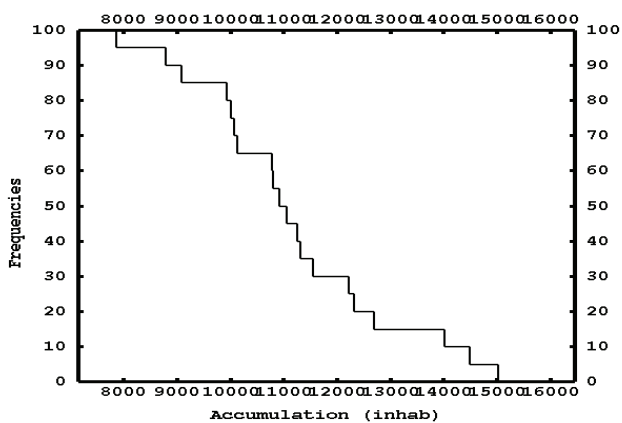


Fig. 7. Risk curve of population exposure to higher than standard levels of nitrate.

slightly underestimated the variogram of realizations. The histogram of data was compared with that of realizations generated by SGS and CCS algorithms (Fig. 10) as another criterion for testing the success of simulations. For this purpose, realizations #1, #5, #10, #15 and #20 were used. As a whole,

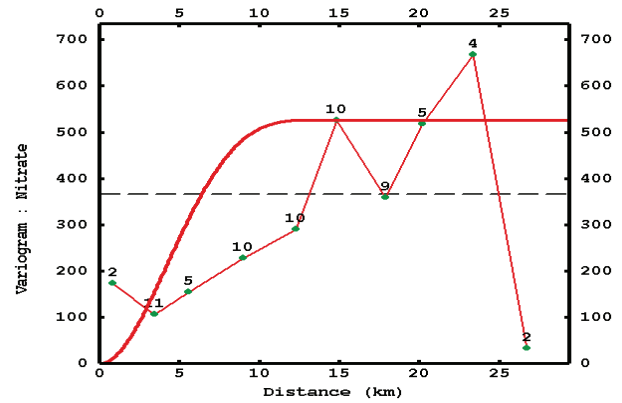


Fig. 8. The model fitted to experimental variogram of nitrate in 2011.

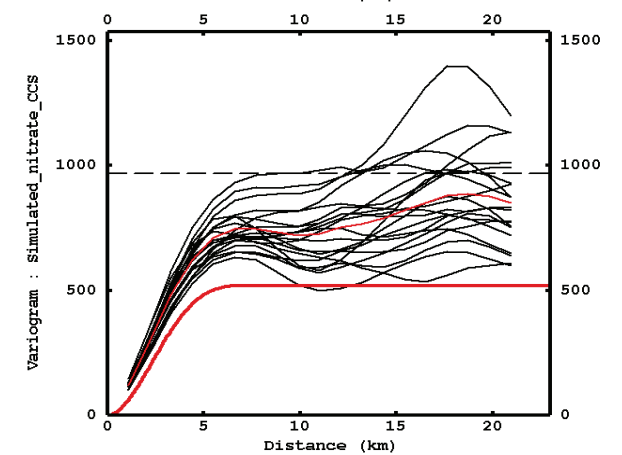
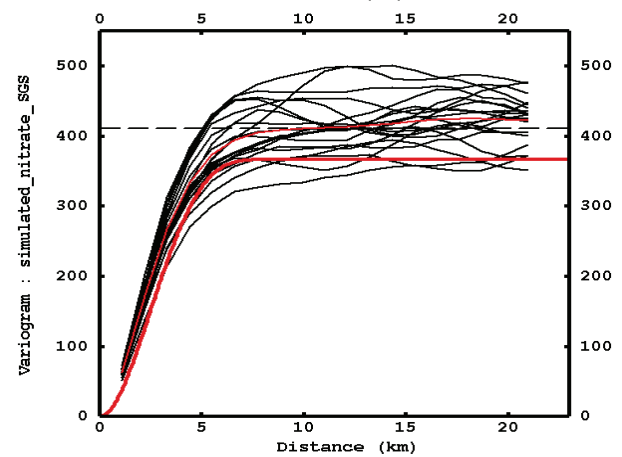


Fig. 9. Experimental variograms of 20 realizations overlaid with that of original variograms for SGS and CCS.

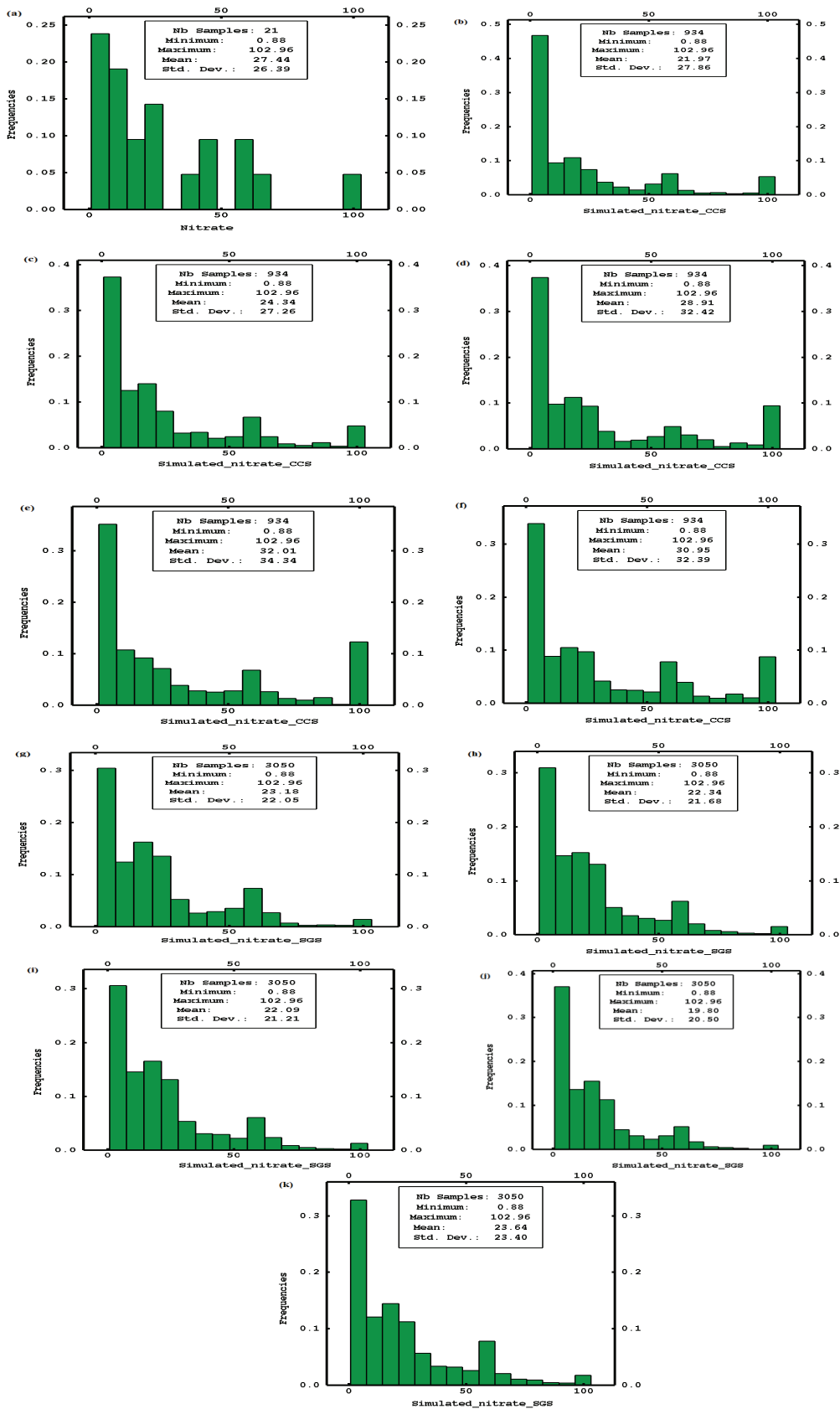


Fig. 10. Histogram of original nitrate in 2011 (a) against the simulated values of nitrate for realizations #1 (b), #5 (c), #10 (d), #15 (e) and #20 (f) by CCS algorithm and the simulated values of nitrate for realizations #1 (g), #5 (h), #10 (i), #15 (j) and #20 (k) by SGS algorithm.

it is clear that realizations produced by SGS have underestimated the mean and standard deviation of data while it has been overestimated through CCS algorithm.

In QQ plots if the quantiles of two populations match each other, the distribution of data would lay along the bisector (e.g., $X = Y$) line. Regarding the obtained QQ plots, it can be concluded that data values have deviated from the bisector line in central and high levels in SGS and also low levels in CCS indicating that SGS has better reproduced the data distribution anyhow (Fig. 11). The standard deviation of realizations was generated through both SGS and CCS to estimate the uncertainty in prediction made by each method (Fig. 12).

It should be noted that in CCS, only collocated secondary data are retained to avoid possible instability in predictions caused by redundant secondary data [24]. Taking this note into account, the uncertainty in predictions of CCS is significantly lower than that of SGS due to extra information of secondary data (e.g., nitrate of 2010). Thereby, the greatest reduction in the estimated standard deviation was located in area with low density of data. Overall, when it comes to uncertainty in spatial predictions, CCS outperforms that of SGS; however, SGS is roughly more accurate than its CCS counterpart in the reproduction of data and their spatial continuity. The results of this paper regarding the reduction in uncertainty of predictions confirm that of earlier studies [24,31]. In this field, Fegh et al. [31] compared SGS and CCS for the prediction of permeability of a gas reservoir in Iran

and concluded that SGS retains original data distribution and, it is more noisy and heterogeneous than CCS which is in agreement with our results. Moreover, Afshari and Shadizadeh [32] emphasized the heterogeneity and exactness property of SGS and the fact that SGS is capable to reproduce the data distribution; however, there was some uncertainty in interpretation of the generated results. In contrast, the randomness of CCS was less than that of SGS.

The land use map produced through imagery analysis has been illustrated in Fig. 13. The overall accuracy of

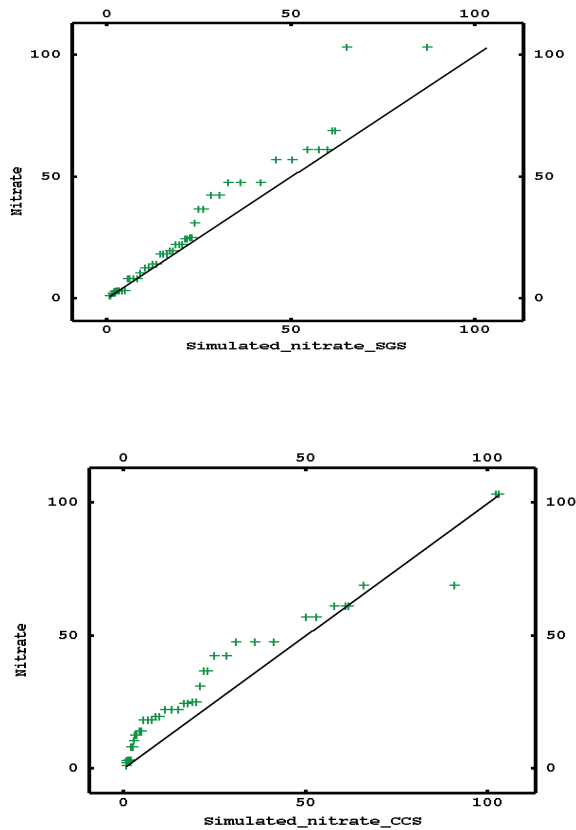


Fig. 11. QQ plot of simulated values using SGS and CCS against that of original nitrate.

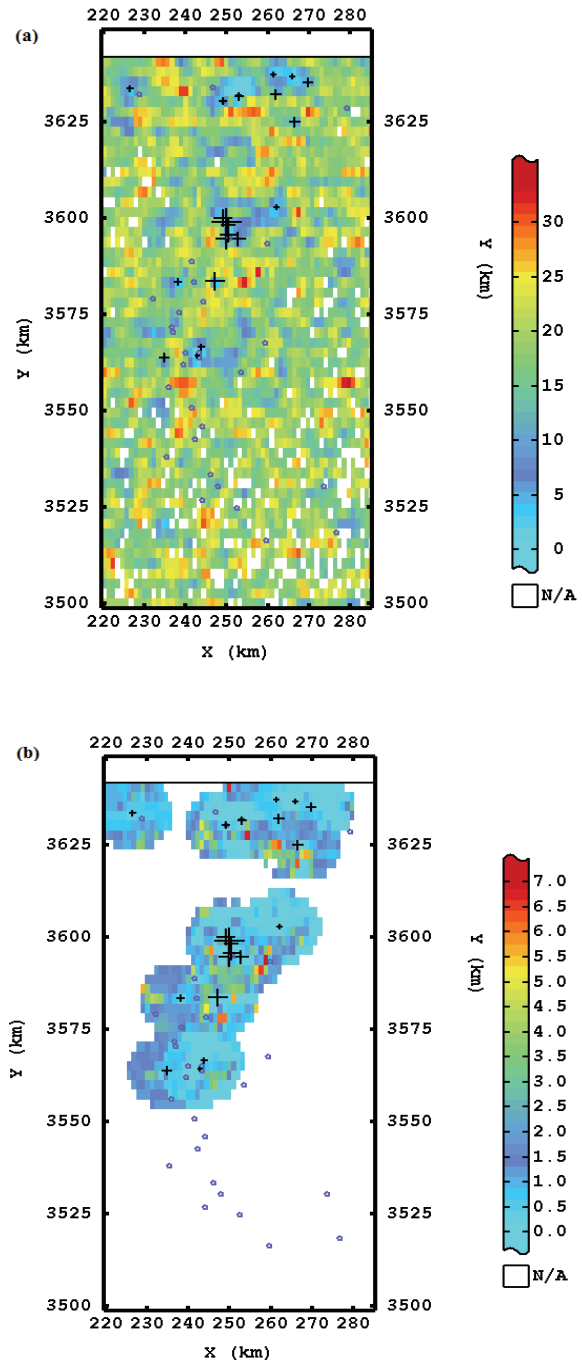


Fig. 12. Standard deviation of simulated values of nitrate generated by SGS (a) and CCS (b).

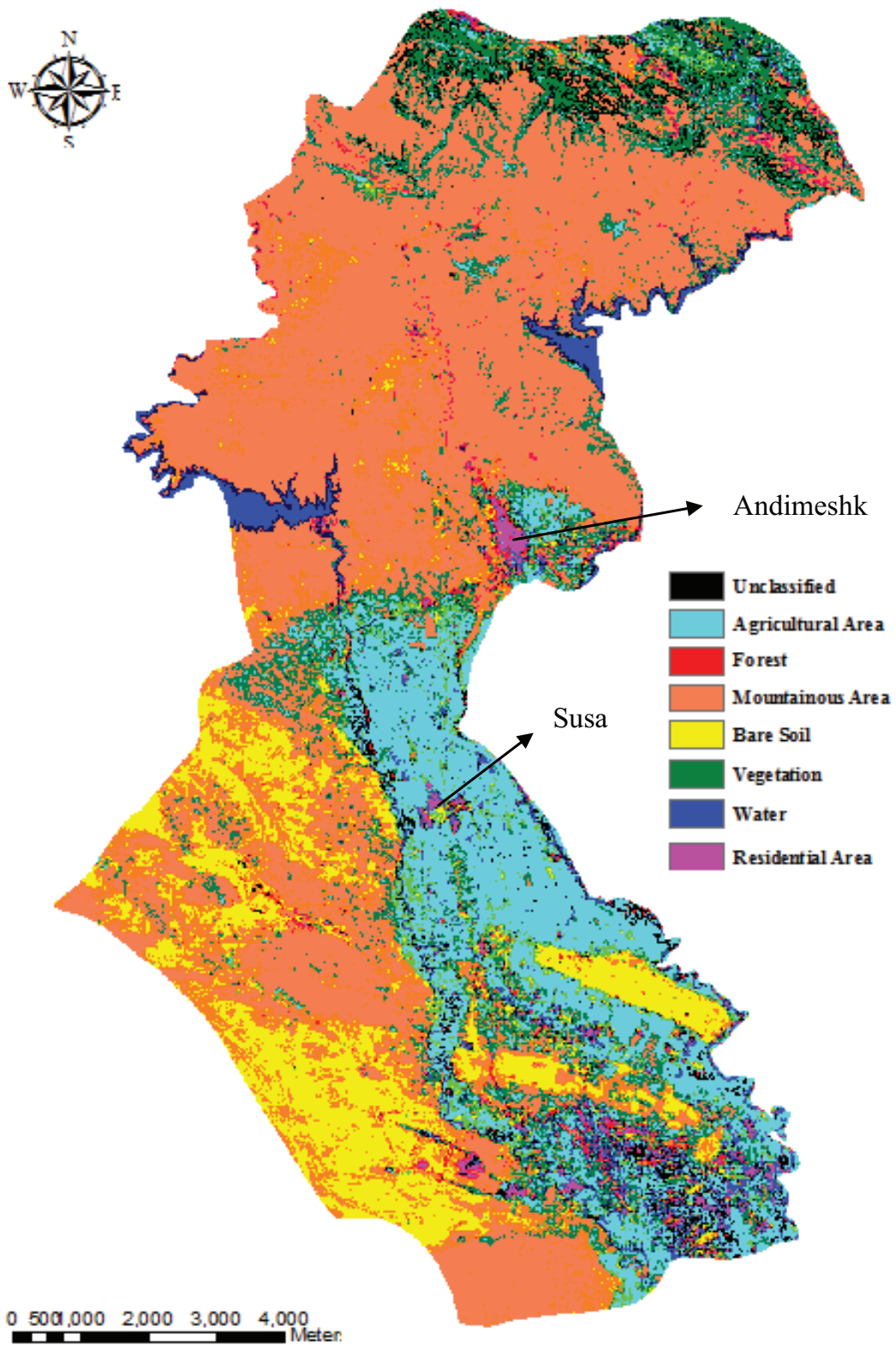


Fig. 13. Land use map of the study area produced by Landsat TM images.

classification results is obtained through division of diagonal elements of confusion matrix (e.g., correctly classified pixels) by the total number of pixels which is 97.07 in this case implying a high level of total accuracy. On the contrary, kappa coefficient is a measure of how the classification results compare with values assigned by chance ranging from 0 to 1. The resultant kappa coefficient was 0.83 confirming the accuracy of the produced land use map. In this case, the main misclassification results belonged to agriculture and bare soil classes with commission (e.g., overestimation) values of 18.15% and 70.48% while the omission (e.g., underestimation) values of these classes were low and equal to 2.98% and 4.00%, respectively. Some of the agricultural fields in the area are not cultivated during July, so, it may be a contributing factor for the confusion between agricultural areas and bare soil. The highest recorded omission value was 14.58% and was associated with water class.

Comparison between the produced land use map and the levels of nitrate recorded between 2010 and 2011 shows that the contribution of residential areas (especially Andimeshk as a major city in the region) has been significant; however, agricultural fields have also played a noticeable role in this respect. There are some high values of nitrate in northern part of the study area which can be attributed to some missing sources such as geological sources that has been recognized as a source of nitrate contamination in other published literatures [42,43]. Contribution of bedrock nitrogen to levels of nitrate in surface and groundwater is a phenomenon which has a great contribution to the total burden of nitrate in some areas. In this field, sedimentary rocks, among other geological formations, include nitrogen as a residual organic matter or as ammonium minerals [44] and are prevalent in the study region, so, the high values of nitrate in this part can possibly be attributed to the geological formations.

4. Conclusion

Uncertainty assessment of simulated values of nitrate through two geostatistical simulation methods namely SGS and CCS was assessed in this study. In summary, when it comes to uncertainty in spatial predictions, CCS outperforms that of SGS; however, SGS is roughly more accurate than its CCS counterpart in reproduction of data and their spatial continuity. The uncertainty in predictions of CCS was significantly lower than that of SGS due to extra information of secondary data (e.g., nitrate of 2010), so, the greatest reduction in the estimated standard deviation of predictions was located in the area with low density of data. One of the shortcomings of this research was related to low number of sampling stations in comparison with the area of the study; however, in CCS only the collocated sampling stations are retained to obviate unwanted uncertainty that may complicate the final analysis of simulation results. Regarding the high cost of water quality monitoring, these simulation techniques can be utilized to compensate for the low data records in area in which there is not enough data to construct a map of contaminated area provided that earlier data set is available to be used as ancillary information.

Considering the land use map of the study area produced by remote sensing imagery, it was concluded that besides residential area and agricultural fields (as the main sources

of nitrate pollution) some geological formations especially in northern part of the region have also contributed to the values of nitrate in the groundwater.

Acknowledgments

The authors are grateful to the help of Andimeshk Health Network and Iran Ministry of Energy. The help of Mr. Eisa Ahmadvpour and Dr. Fatemeh Mehrabi Sharafabadi in field studies and data processing is also greatly appreciated.

References

- [1] K. Rina, P.S. Datta, C.K. Singh, S. Mukherjee, Determining the genetic origin of nitrate contamination in aquifers of Northern Gujarat, India, *Environ. Earth Sci.*, 71 (2014) 1711–1719.
- [2] T. Opazo, R. Aravena, B. Parker, Nitrate distribution and potential attenuation mechanisms of a municipal water supply bedrock aquifer, *Appl. Geochem.*, 73 (2016) 157–168.
- [3] J. L'hirondel, *Nitrate and Man: Toxic, Harmless or Beneficial?* CABI Publishing, New York, USA, 2002.
- [4] B.T. Nolan, Relating nitrogen sources and aquifer susceptibility to nitrate in shallow ground waters of the United States, *Ground Water*, 39 (2001) 290–299.
- [5] A.Y.R. Fabro, J.G.P. Avila, M.V.E. Alberich, S.A.C. Sansores, M.A. Camargo-Valero, Spatial distribution of nitrate health risk associated with groundwater use as drinking water in Merida, Mexico, *Appl. Geochem.*, 65 (2015) 49–57.
- [6] T.A. Evans, D.R. Maidment, A Spatial and Statistical Assessment of the Vulnerability of Texas Groundwater to Nitrate Contamination, CRWR Online Report 95–2, Centre for Research in Water Resources, University of Texas at Austin, 1995.
- [7] ATSDR, The Priority List of Hazardous Substances That Will Be the Subject of Toxicological Profiles, Agency for Toxic Substances and Disease Registry, 2011.
- [8] E. Moore, E. Matalon, C. Balazs, J. Clary, L. Firestone, S. De Anda, M. Guzman, The Human Costs of Nitrate-Contaminated Drinking Water in the San Joaquin Valley, Pacific Institute, Oakland, CA, 2011.
- [9] J. Wongsanit, P. Teartisup, P. Kerdsueb, P. Tharnpoophasiam, S. Worakhunpiset, Contamination of nitrate in groundwater and its potential human health: a case study of lower Mae Klong river basin, Thailand, *Environ. Sci. Pollut. Res.*, 22 (2015) 11504–11512.
- [10] J.Y. Cheong, S.-Y. Hamm, J.H. Lee, K.S. Lee, N.C. Woo, Groundwater nitrate contamination and risk assessment in an agricultural area, South Korea, *Environ. Earth Sci.*, 66 (2012) 1127–1136.
- [11] R. Sadler, B. Maetam, B. Edokpolo, D. Connell, J. Yu, Health risk assessment for exposure to nitrate in drinking water from village wells in Semarang, Indonesia, *Environ. Pollut.*, 216 (2016) 738–745.
- [12] J. Wu, Z. Sun, Evaluation of shallow groundwater contamination and associated human health risk in an alluvial plain impacted by agricultural and industrial activities, mid-west China, *Exposure Health*, 8 (2016) 311–329.
- [13] Y. Zhou, A. Wei, J. Li, L. Yan, J. Li, Groundwater quality evaluation and health risk assessment in the Yinchuan Region, northwest China, *Exposure Health*, 8 (2016) 443–456.
- [14] R. Mirzaei, M. Sakizadeh, Comparison of interpolation methods for the estimation of groundwater contamination in Andimeshk-Shush Plain, Southwest of Iran, *Environ. Sci. Pollut. Res.*, 23 (2016) 2758–2769.
- [15] M. Qu, W. Li, C. Zhang, Assessing the risk costs in delineating soil nickel contamination using sequential Gaussian simulation and transfer functions, *Ecol. Inf.*, 13 (2013) 99–105.
- [16] M. Jalali, S. karami, A. Fatehi Marj, Geostatistical evaluation of spatial variation related to groundwater Quality Database: case study for Arak Plain aquifer, Iran, *Environ. Model. Assess.*, 21 (2016) 707–719.

- [17] E. Guastaldi, A.A. De Frate, Risk analysis for remediation of contaminated sites: the geostatistical approach, *Environ. Earth Sci.*, 65 (2012) 897–916.
- [18] B. Sadeghi, N. Madani, E.J.M. Carranza, Combination of geostatistical simulation and fractal modeling for mineral resource classification, *J. Geochem. Explor.*, 149 (2015) 59–73.
- [19] V. D'Agostino, E.A. Greene, G. Passarella, M. Vurro, Spatial and temporal study of nitrate concentration in groundwater by means of coregionalization, *Environ. Geol.*, 36 (1998) 285–295.
- [20] S. Rouhani, T.J. Hall, Space and Time Kriging of Groundwater Data, M. Armstrong, Ed., *Geostatistics*, 2nd ed., Kluwer, Dordrecht, 1988, pp. 639–651.
- [21] P. Goovaerts, P.H. Sonnet, Study of Spatial and Temporal Variations of Hydrogeochemical Variables Using Factorial Kriging Analysis, A. Soares, Ed., *Geostatistics Troia'92*, Kluwer, Dordrecht, 1992, pp. 745–756.
- [22] X. Liang, K. Schilling, Y.K. Zhang, C. Jones, Co-kriging estimation of nitrate-nitrogen loads in an agricultural river, *Water Resour. Manage.*, 30 (2016) 1771–1784.
- [23] H. Wackernagel, *Multivariate Geostatistics: An Introduction with Applications*, 3rd ed, Springer, New York, 2003.
- [24] H. Bourennane, D. King, A. Couturier, B. Nicoullaud, B. Mary, G. Richard, Uncertainty assessment of soil water content spatial patterns using geostatistical simulations: an empirical comparison of a simulation accounting for single attribute and a simulation accounting for secondary information, *Ecol. Modell.*, 205 (2007) 323–335.
- [25] M. Sakizadeh, F. Faraji, M.J. Pouraghiyayi, Quality of groundwater in an area with intensive agricultural activity, *Exposure Health*, 8 (2016) 93–105.
- [26] APHA, *Standard Methods for the Examination of Water and Wastewater*, 21st ed., Washington, D.C., USA, 1996.
- [27] USEPA, *Human Health Risk Assessment Protocol*, 2005. Available at: <http://www.epa.gov/osw/hazard/tsd/td/combust/finalmact/ssra/05hhrap7.pdf>
- [28] A. Castrignanò, A. Buondonno, P. Odierna, C. Fiorentino, E. Coppola, Uncertainty assessment of a soil quality index using geostatistics, *Environmetrics*, 20 (2009) 298–311.
- [29] J.P. Chilès, P. Delfiner, *Geostatistics: Modelling Spatial Uncertainty*, Wiley, New York, 1999.
- [30] M. Abzalov, *Applied Mining Geology*, Springer, Switzerland, 2016.
- [31] A. Fegh, M.A. Riahi, G.H. Norouzi, Permeability prediction and construction of 3D geological model: application of neural networks and stochastic approaches in an Iranian gas reservoir, *Neural. Comput. Appl.*, 23 (2013) 1763–1770.
- [32] A. Afshari, S.R. Shadizadeh, Integration of petrophysical and seismic data to construct a reservoir permeability model, *Energy Sources Part A*, 37 (2015) 679–686.
- [33] A.S. Almeida, A.G. Journel, Joint simulation of multiple variables with a Markov-type coregionalization model, *Math. Geol.*, 26 (1996) 565–588.
- [34] C. Song, C.E. Woodcock, K.C. Seto, M.P. Lenney, S.A. Macomber, Classification and change detection using Landsat TM data: when and how to correct atmospheric effects? *Remote Sens. Environ.*, 75 (2001) 230–244.
- [35] C. Lin, C.C. Wu, K. Tsogt, Y.C. Ouyang, C.I. Chang, Effects of atmospheric correction and pansharpening on LULC classification accuracy using WorldView-2 imagery, *Inf. Process. Agric.*, 2 (2015) 25–36.
- [36] M.J. Canty, *Image Analysis, Classification, and Change Detection in Remote Sensing: With Algorithms for ENVI/IDL*, 3rd ed., CRC Press, USA, 2014.
- [37] R.G. Congalton, A review of assessing the accuracy of classifications of remotely sensed data, *Remote Sens. Environ.*, 37 (1991) 35–46.
- [38] U.A. Mueller, J. Ferreira, The U-WEDGE transformation method for multivariate geostatistical simulation, *Math. Geosci.*, 44 (2012) 427–448.
- [39] Y.P. Lin, T.K. Change, T.P. Teng, Characterization of soil lead by comparing sequential Gaussian simulation, simulated annealing simulation and kriging methods, *Environ. Geol.*, 41 (2001) 189–199.
- [40] M. Asefi, F. Radmanesh, H. Zarei, Vulnerability Assessment of Andimeshk Plain Using Drastic Model Coupled with AHP Method, First National Conference on Planning and Conservation of Environment, in Persian, 1996.
- [41] P. Goovaerts, Geostatistical approaches for incorporating elevation into the spatial interpolation of rainfall, *J. Hydrol.*, 228 (2000) 113–129.
- [42] M. Lowe, J. Wallace, Evaluation of Potential Geologic Sources of Nitrate Contamination in Ground Water, Cedar Valley, Iron County, Utah, with Emphasis on the Enoch Area, Utah Geological Survey Special Study 100, 2001.
- [43] S. Stadler, K. Osenbruck, K. Knoller, A. Suckowa, J. Sulzenfub, H. Oster, T. Himmelsbach, H. Hotzl, Understanding the origin and fate of nitrate in groundwater of semi-arid environments, *J. Arid Environ.*, 72 (2008) 1830–1842.
- [44] J.M. Holloway, R.A. Dahlgren, B. Hansen, W.H. Casey, Contribution of bedrock nitrogen to high nitrate concentrations in stream water, *Nature*, 395 (1998) 785–788.